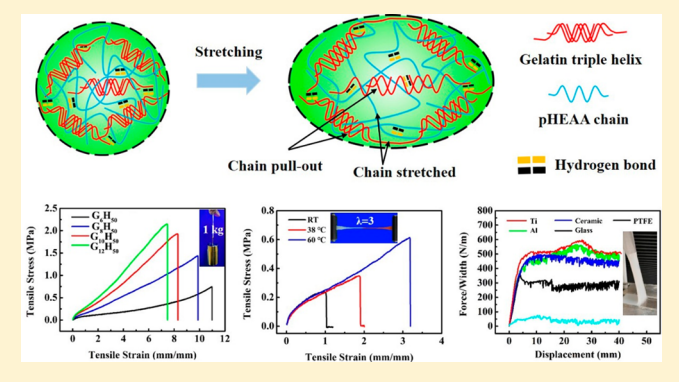


Double-Network Physical Cross-Linking Strategy To Promote Bulk Mechanical and Surface Adhesive Properties of Hydrogels

Li Tang, †,‡,||,⊥ Dong Zhang, ||,⊥ Liang Gong, † Yanxian Zhang, || Shaowen Xie,‡, || Baiping Ren, || Yonglan Liu, || Fengyu Yang, || Guiyin Zhou, † Yung Chang, * Jianxin Tang,*,† and Jie Zheng*, || •

Supporting Information

ABSTRACT: Development of mechanically strong and adhesive hydrogels with self-recovery and self-healing properties is important for many applications but has proven to be very challenging. Here, we reported a double-network design strategy to synthesize a fully physically cross-linked doublenetwork (DN) hydrogel, consisting of the first gelatin network and the second poly(N-hydroxyethyl acrylamide) network where both networks were mainly cross-linked by hydrogen bonds. The resultant gelatin/pHEAA hydrogels exhibited high mechanical property (tensile stress of 1.93 MPa, tensile strain of 8.22, tearing energy of 4584 J/m²), fast self-recovery at room temperature (toughness/stiffness recovery of 70.2%/ 68.0% after 10 min resting), and good self-healing property



(self-healed tensile stress/strain of 0.62 MPa/3.2 at 60 °C for 6 h). More importantly, gelatin/pHEAA hydrogels also exhibited strong surface adhesion on different hydrophilic solid surfaces, as indicated by high adhesion energy (i.e., interfacial toughness) of 645 J/m² on glass, 867 J/m² on Al, 702 J/m² on Ti, and 579 J/m² on ceramics. Surface adhesion can be largely retained after multiple, repeatable adhere on/peel off actions. Reversible and strong mechanical properties in bulk and on solid surfaces are likely attributed to reversible hydrogen bondings and physical coordinate bonds between the networks and between networks and surfaces. This work demonstrates our design principle that multiple physical bonds in both networks offer excellent mechanical recoverability, self-healing, and self-adhesive properties, while DN structure provides strong and tough mechanical properties via efficient energy dissipation by sacrificed bonds, which offers a new possibility to develop next-generation hydrogels with desirable properties used for soft robotics, wearable electronics, and human-machine interfaces.

■ INTRODUCTION

Polymer hydrogels as soft-wet materials have been extensively studied and used in many scientific research and industrial applications, including soft robotics, 1-3 wearable electronics, $^{4-6}$ and cartilage tissue scaffolds, $^{7-9}$ due to their unique structure-dependent properties, i.e., high water content, 3D polymer network, swelling behavior, and biomimetics. However, most polymer hydrogels are mechanically weak and lack fatigue resistance, self-recovery, and/or self-healing properties, which severely limit their widespread applications. To address those issues, many different tough hydrogels have been developed to improve their mechanical limits, such as nanocomposite (NC) gels, 10-12 hybrid hydrogels, 13,14 and double-network (DN) hydrogels. 15,16 Generally, these tough hydrogels can achieve the tensile strength of >1 MPa and toughness of >1000 J/m².

Particularly, DN hydrogels contain two independent, contrasting, and interpenetrating networks, which offer different selections and combinations of different polymers and cross-linkers to construct a double-network network with multiple energy dissipation mechanisms for enhancing mechanical properties and multiple functionality for achieving self-recovery and self-healing properties. Such unique twonetwork structures enable DN hydrogels to achieve very high mechanical properties, e.g., tensile stress of 1-10 MPa, compression stress of 20-60 MPa, and fracture energy of 1000 J/m^{2.17} However, challenges still remain. First, most DN hydrogels are chemically cross-linked in either network, so the large deformation of these hydrogels often causes the

Received: August 15, 2019 Revised: November 16, 2019 Published: December 12, 2019



[†]Hunan Key Laboratory of Biomedical Nanomaterials and Devices College of Life Sciences and Chemistry and [‡]College of Packaging and Material Engineering, Hunan University of Technology, Zhuzhou 412007, China

[§]Department of Chemical Engineering R&D Center for Membrane Technology, Chung Yuan Christian University, Taoyuan 320, Taiwan

Department of Chemical, Biomolecular, and Corrosion Engineering, The University of Akron, Akron, Ohio 44325, United States

irreversible and permanent breakage of covalent bonds, resulting in the loss or lack of self-recovery/healing properties. To overcome this issue, a common strategy is to introduce physical and reversible bonds (e.g., hydrogen bond, 18,19 hydrophobic association, 20,21 ionic association 22,23) into either one or both networks to produce hybrid chemically and physically cross-linked DN hydrogels or fully physically crosslinked DN hydrogels, which realize self-recovery and selfhealing properties, while still retaining comparable mechanical strength and toughness to chemically cross-linked DN hydrogels. Second, it is also well noted that no two polymers are compatible to each other to gelate and form DN hydrogels. Currently, only several physical-based DN hydrogels have been reported to possess both mechanically strong and recovery properties, including hybrid DN hydrogels of agar/PAAm, 15,24 gelatin/PAAm,²⁵ BSA/PAAm,²⁶ chitosan/PAAm,²⁷ PVA/PAAm,²⁸ PVA/P(AAm-co-SBMA),²⁹ K⁺/guanosine/ PDMAAm,³⁰ Ca²⁺/alginate/PAAm,²³ Ca²⁺/IC/PAAm and Ca²⁺/KC/PAAm,³¹ K⁺/KC/PAAm,³² Fe³⁺/pectin/PAAm,³³ agar/P(AAm-co-AAc)/Fe³⁺,³⁴ La³⁺/cholate/PAAm,³⁵ SO₄²⁻/chitosan/PAAm,³⁶ B(OH)₄⁻/HPG/PAAm,³⁷ and fully physical cross-linked DN hydrogels of agar/PHEAA,¹⁸ agar/ PAAEE, Pagar/PAAm, PVA/PAAc, PVA/P(AAm-co-AAc), PU/DHIR, agar/P(AAm-co-SMA), RAM-co-SMA), RAM-co (Table S1).

More importantly, among those physical-based hydrogels, only few hydrogels possess strong bulk toughness capacity with strong interfacial toughness of 650-7000 J/m². This indicates that not all tough hydrogels are surface adhesive to solid surfaces, or vice versa, presumably because interfacial toughness stems from different intermolecular interactions. From a design viewpoint of DN hydrogels, the synthesis of fully physical DN hydrogels with both strong bulk and interfacial toughness is far more challenging than those of chemical-based DN hydrogels because the latter systems could achieve toughness via chemical links both within two networks and between networks and solid surfaces. Very few fully physical cross-linked DN hydrogels have been developed and demonstrated both bulk toughness and interfacial toughness. For instance, a fully physical Agar/pHEAA DN hydrogel, cross-linked by hydrogen bonds in both networks, achieved high both bulk toughness of ~8000 J/m² and interfacial toughness of $\sim 2000-7000 \text{ J/m}^2$, as well as toughness/stiffness recovery of 62%/30% and certain degree of self-healing property. 18 Another Agar/pAAEE DN physical hydrogel also demonstrated bulk toughness of 1612 J/m², interfacial toughness of 400-650 J/m², and toughness/stiffness recovery of 90%/91%. 19

Herein, we designed, synthesized, and characterized a new fully physically linked gelatin/pHEAA DN hydrogel, consisting of a gelatin gel and a poly(N-hydroxyethyl acrylamide) (pHEAA) gel as the first and second physical networks. Gelatin as a mixture of soluble proteins is often prepared by partial hydrolysis of skin, bone, cartilage, and connective tissues and proved its excellent biocompatibility, good cell/tissue affinity, and low toxicity. S1,52 Both gelatin and pHEAA contain many hydrophilic functional groups of -OH, $-NH_2$, and $-COO^-$, allowing them to form massive hydrogen bonds between and within the two networks. Thus, both networks

were designed to be physically cross-linked by hydrogen bonds. Moreover, gelatin is a thermoreversible material but with a low melt temperature (26–30 °C) as compared to that of agar (85–95 °C). Similar to agar, gelatin undergoes a structural change from random coils in a sol state at 60 °C to triple helix in a gel state at 25 °C. More importantly, a systematic mechanical comparison among gelatin-based hydrogels in Figure 1 showed that except for hybrid gelatin—nanocomposite

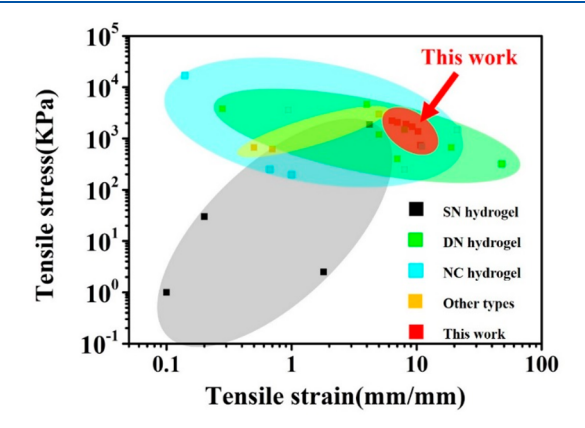


Figure 1. Systematic comparison of tensile stress and tensile strain among different types of gelatin-based hydrogels, including gelatin/pHEAA DN hydrogel in this work, gelatin SN hydrogels, ^{53–56} gelatin-based DN hydrogels, ^{25,57–61} gelatin-based NC hydrogels, ^{52,57,62–65} and others. ^{66–68}

hydrogels, most gelatin-based hydrogels exhibited low mechanical properties as evidenced by low tensile stress of 1-1000 KPa and low tensile strain of 0.1-5. Different from these mechanically weak gelatin-based hydrogels, our gelatin/ pHEAA DN bulk hydrogels exhibited high mechanical properties (elastic modulus of 0.52 MPa, tensile stress of 1.93 MPa at a failure strain of 8.22, and toughness of 4584 J/ m²), fast toughness/stiffness self-recovery of 70.2%/68.0% after 10 min resting at room temperature without any external stimuli, and good self-healing property with self-healed stress/ strain of 0.62 MPa/3.2 at 60 °C for 6 h. More importantly, without any surface modification, gelatin/pHEAA hydrogels can also readily adhere to different nonporous solid surfaces including glass, titanium, aluminum, ceramics, and poly-(tetrafluoroethylene), with strong interfacial toughness of 580–867 J/m² (except for poly(tetrafluoroethylene)). Overall, our design principle for this gelatin/pHEAA hydrogel demonstrates that multiple physical bonds in both networks offer excellent mechanical recoverability, self-healing, and selfadhesive properties, while DN structure provides strong and tough mechanical properties via efficient energy dissipation by sacrificed bonds. Thus, different from most gelatin-based hydrogels, our gelatin/pHEAA DN gels demonstrated the integrated multiple functions of strong bulk and interfacial toughness, fast mechanical recovery, and good self-healing properties, in which design strategy, hydrogel systems, and their structure-property relationship could offer valuable insights into next-generation soft materials for wearable electronic devices, human-machine interfaces, and cartilage tissue scaffolds.

■ MATERIALS AND METHODS

Materials. Gelatin (type A and gel strength \sim 300 g bloom) and 2-hydroxy-4'-(2-hydroxyethoxy)-2-methylpropiophenone (Irgacure

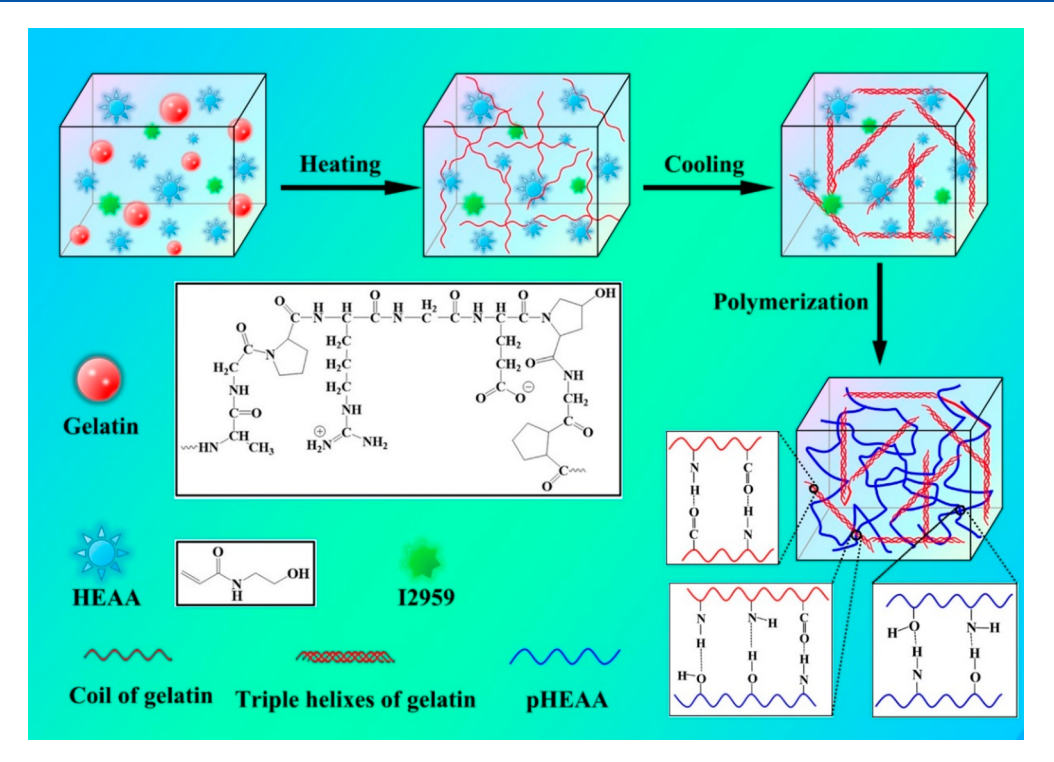


Figure 2. Schematic of a one-pot synthesis of a fully physically cross-linked gelatin/pHEAA DN hydrogel, where inter- and intranetworks are cross-linked by hydrogen bonds.

2959) were purchased from Sigma-Aldrich (Milwaukee, WI). N-Hydroxyethyl acrylamide (HEAA, >98%) was purchased from TCI America. Deionized water used in this study was purified by a Millipore water purification system with a resistivity of 18.2 M Ω cm.

Hydrogel Synthesis. The fully physically linked gelatin/HEAA DN hydrogels were synthesized using a one-pot heating-coolingphotopolymerization method as previously reported. 18 Briefly, all reactants of HEAA (50 wt %), gelatin (10 wt %), initiator Irgacure 2959 (1 mol % of HEAA), and deionized water (40 wt %) were added into a bottle. The bottle was sealed and degassed three times with stirring and then gradually heated up to 60 °C in a water bath to dissolve all reactants, forming a transparent precursor solution. Next, the solution was injected into a glass mold with a 1 mm thick Teflon spacer and gradually cooled down to room temperature. During the cooling process, gelatin formed the first physically cross-linked network via the association of triple helix. Then, the mold was placed under UV light (8 W, 365 nm) for 1 h to form the second physically cross-linked network of pHEAA via hydrogen bond that interpenetrated with the first gelatin network. After polymerization, the mold was stored in a 4 °C refrigerator for 15 min in order to strengthen gelatin from the first network. Gels were removed from the mold, and the as-prepared samples were used for mechanical tests.

Mechanical Tests. *Tensile Test.* The tensile tests were performed on a universal tester (Instron 3345, MA) equipped with a 500 N load cell at 100 mm/min speed. Gel samples were cut into dumbbell shape (ASTM-638-V) with a gauge length of 25 mm, width of 3.18 mm, and thickness of 1 mm. The tensile strain (ε) was the elongation of the sample (Δl) divided by its initial length (l_0) $(\varepsilon = \Delta l/l_0)$. The tensile stress (σ) was the load force (F) divided by the original cross-sectional area (A_0) of the specimen $(\sigma = F/A_0)$. The elastic modulus (E) was calculated in the initial linear range (0.1%-10%) from the tensile stress/strain curves.

Hysteresis Tests. Specimens were stretched to a varied strain at rate of 100 mm/min and then unloaded to the strain of 0 at the same rate. Dissipated energy was calculated from the area between the loading—unloading curves. The successive loading—unloading test was performed on the same hydrogel. To avoid or decrease water loss during recovery test, a thin layer of grease was applied on the gel surface.

Tearing Tests. The hydrogel sample with trousers shape (40 mm/min length, 25 mm in width, and 1 mm in thickness) and an initial notch of 20 mm was used to test tearing energy. One arm of the hydrogel sample was clamped and fixed, while the other one was clamped and pulled up at a rate of 100 mm/min. The tearing energy (T) is defined as the work required to tear a unit area and estimated by $T=2F_{\rm max}/\omega$, where $F_{\rm max}$ is the force of peak values during tearing test and ω is the thickness of the sample.

Peeling Tests. To form a tough bonding interface of hydrogel on nonporous substrates, the solid substrates were sequentially cleaned with acetone, ethanol, and water in ultrasound machines for 30 min and dried in an oven. Then the hydrogel sample was prepared on clean substrates with a Teflon spacer (16.5 mm × 65 mm × 3 mm). For easier demolding, a clear PET film was used to cover the upside of the mold. The following hydrogel was prepared with the same process as mentioned above. Before the test, 3 M tape had been adhered to the top of hydrogel. Then the gel samples were tested with a standard 90° peeling test setup under different peel rates according to the test need. The interfacial toughness (g) was estimated by $g = F_{\rm max}/w$, where $F_{\rm max}$ is the maximum force in the peeling process and w is the width of the tested hydrogel sheet.

Self-Healing Tests. Hydrogel specimens were cut into two pieces, and the fresh cutting surfaces were coated with water and put together. The contacted hydrogel specimens were placed in the mold and covered by glasses. The mold was further placed in a sealed plastic bag and kept in air moisture under different temperatures and times. Tensile tests of the healed hydrogels were performed at the same conditions.

Self-healing efficiency was defined and estimated by an equation of

self-healing efficiency = $\sigma_0/\sigma_t \times 100\%$

where σ_0 is a tensile stress of the original gel, while σ_t is a tensile stress of the self-healed gel under different temperatures or different times.

Swelling Test. Hydrogel specimens were fully and separately immersed in water, urea solution (5 M), and NaSCN solution (5 M). After the excess surface water of swollen DN hydrogels was carefully removed, samples were weighed before and after the swelling; thus, the swelling ratio (SR) of DN gel was calculated by an equation of SR

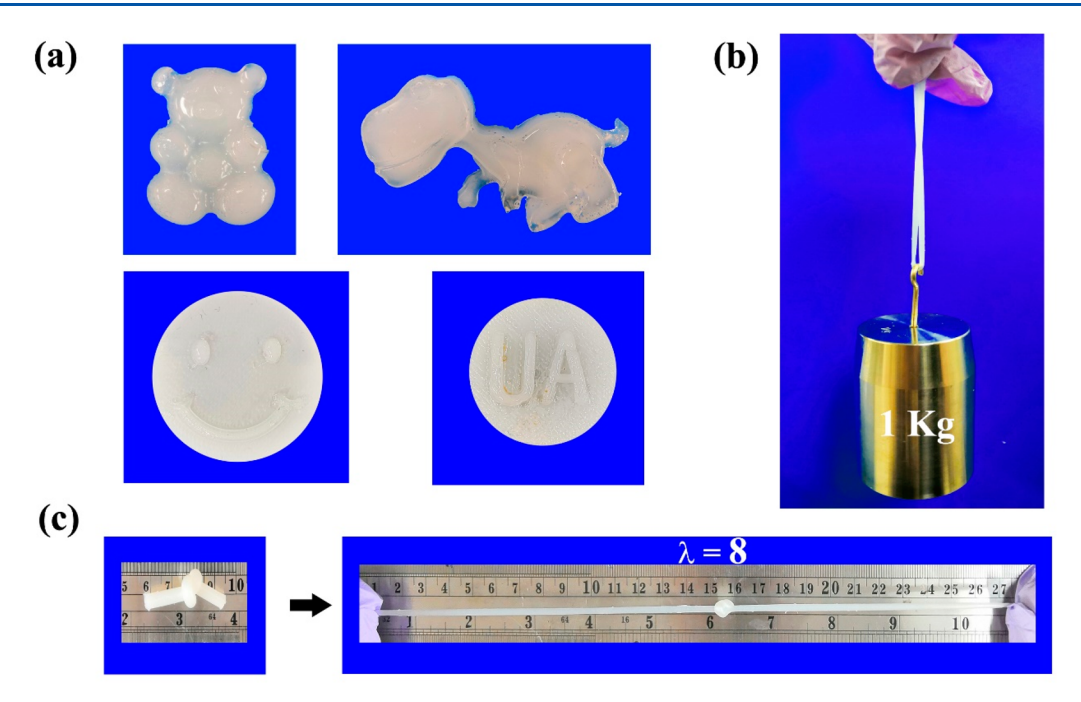


Figure 3. Visual inspection of mechanical properties of gelatin/pHEAA DN hydrogel. Gelatin/pHEAA hydrogel can (a) adapt different shapes of teddy bear, dinosaur, smiley face, and UA logo, (b) lift 1 kg weight, and (c) withstand knot stretching up to 8 times of its original length.

 $(g/g) = (m_t - m_0)/m_0$, where m_t is the weight of swollen hydrogel at t h and m_0 is the initial weight of the same hydrogel before swelling.

Fourier Transform Infrared Spectroscopy (FT-IR). Infrared spectroscopy of dried sheet gelatin SN gel, pHEAA SN gel, and gelatin/pHEAA DN gel was carried out by using a Fourier transform infrared spectrophotometer (Nicolet 6700).

Scanning Electron Microscopy (SEM). The morphology and microscopy of hydrogels were checked by a field emission scanning electron microscope (TESCAN MIRA3 LMU). All hydrogel samples were frozen by liquid nitrogen at $-196\ ^{\circ}\mathrm{C}$ and dried in a freeze drier. Before tests, all hydrogel samples were coated with a thin layer of platinum.

■ RESULT AND DISCUSSION

Synthesis and Structural Characterization of Gelatin/ pHEAA DN Gels. Figure 2 shows a heating-coolingphotopolymerization method to prepare the fully physically linked gelatin/pHEAA DN hydrogels. Briefly, all reactants including gelatin, monomer HEAA, and UV initiator I2959 were well mixed together in DI water. The mixture solution was first heated to 60 °C to dissolve gelatin, followed by the cooling process to room temperature, during which gelatin underwent a conformational change from random coils at 60 °C to triple-helix bundles at room temperature. Then, UV light was introduced to initiate and polymerize the second network of pHEAA, which was interpenetrated with the first gelatin network, finally producing gelatin/pHEAA DN hydrogels with a milky white color. During the whole gelation process, no chemical cross-linker was introduced to the gelatin/pHEAA hydrogel, so both networks are physically cross-linked by reversible noncovalent bonds, i.e., hydrogen bonds, van der Waals interactions, and chain entanglements.

At first glance, gelatin/pHEAA DN gels were not only sufficiently flexible to fabricate any complex 3D shape, including teddy bear, dinosaur, smiley face, and UA logo (abbreviation of The University of Akron) (Figure 3a) but also strong enough to lift a 1 kg weight (Figure 3b) and withstand knot stretching up to ≈ 8 times of its original length (Figure

3c). Figure 4a shows FT-IR spectra to characterize and compare the chemical structure of gelatin SN, pHEAA SN, and

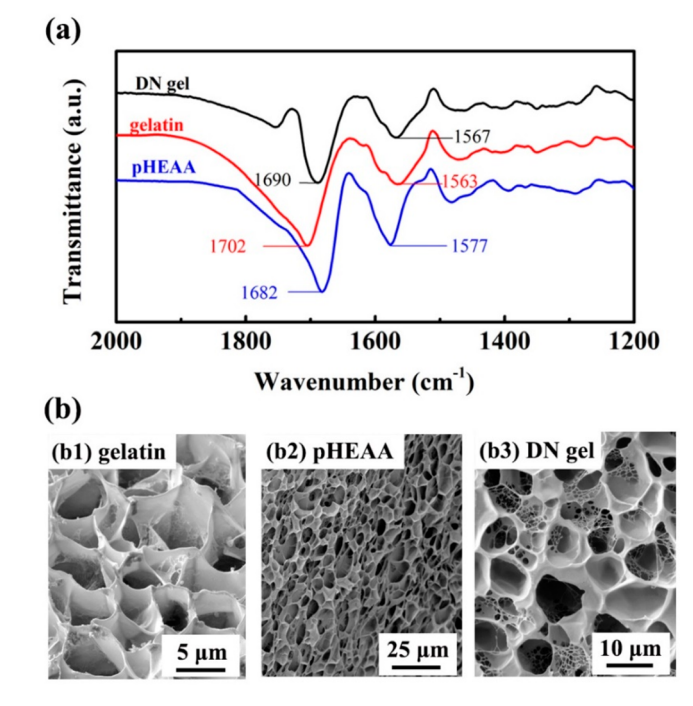


Figure 4. Structural characterization of gelatin SN hydrogel, pHEAA SN hydrogel, and $G_{10}H_{50}$ gelatin/pHEAA DN hydrogel by (a) FT-IR spectra and (b) SEM.

gelatin/pHEAA DN hydrogels. Gelatin SN hydrogel exhibited two characteristic peaks at 1702 and 1563 cm $^{-1}$ corresponding to stretching vibration of C=O and bending vibration of N-H from amide, respectively. Since pHEAA has different molecular structure from gelatin, the characteristic peaks of C=O and N-H from amide were shifted to \sim 1682 and

~1577 cm⁻¹, respectively. Additionally, when the two gelatin and pHEAA networks are interpenetrated together, the formation of hydrogen bonds between the two networks will also affect the local environments and peak locations of C=O at 1690 cm⁻¹ and N-H at 1567 cm⁻¹. This also indicates from another viewpoint that only hydrogen bonds, but no new chemical bonds, are formed between the two networks in gelatin/pHEAA DN gels.

In parallel, SEM images further showed that gelatin SN gel had more uniform pore structures with the pore sizes of $3-7~\mu m$ (Figure 4b1), while pHEAA SN gel had loose pore structure with relatively larger pore sizes of $4-14~\mu m$ (Figure 4b2). Different from either SN gel, gelatin/pHEAA DN gel clearly presented the mixed pore structures, confirming the interpenetrating networks by both gelatin and pHEAA (Figure 4b3). Visual inspection of different porous structures among the three hydrogels suggests that such heterogeneous network structure may be caused by the physical association and entanglement of gelatin and pHEAA chains, which further enhanced network interactions between and within the two networks.

High Mechanical Properties of Gelatin/pHEAA DN Gels. Considering that gelatin/pHEAA DN gel was only physically cross-linked by the first gelatin network and the second pHEAA network, it is interesting and important to reveal the effects of both network components on mechanical properties of gelatin/pHEAA DN gels. To end this, we prepared different gelatin/pHEAA DN gels by varying the concentrations of gelatin from 6 to 12 wt % and HEAA from 30 to 60 wt % for tensile tests (Table 1).

Table 1. Compositional and Mechanical Properties of Gelatin/pHEAA DN Hydrogels

sample	gelatin (wt %)	HEAA (wt %)	water (wt %)	tensile stress (MPa)	tensile strain (mm/mm)
G_6H_{50}	6	50	44	0.74	10.74
G_8H_{50}	8	50	42	1.44	9.86
$G_{10}H_{50}$	10	50	40	1.93	8.22
$G_{12}H_{50}$	12	50	38	2.06	7.01
$G_{10}H_{30}$	10	30	60	0.74	5.22
$G_{10}H_{40}$	10	40	50	1.74	9.05
$G_{10}H_{60}$	10	60	30	2.33	6.21

First, regarding the gelatin effect, Figure 5a1 shows the tensile stress-strain curves of gelatin/pHEAA DN gels prepared at different gelatin concentrations of 6-12 wt % and a constant HEAA concentration of 50 wt %. It can be seen that as the gelatin concentration increased from 6 to 12 wt %, gelatin/pHEAA DN gels increased their tensile stress from 0.74 to 2.06 MPa and elastic modulus from 0.19 to 0.64 MPa but decreased the corresponding tensile strain from 10.74 to 7.01 mm/mm. It appears that the higher concentration of gelatin makes gelatin/pHEAA hydrogels stronger but more brittle, consistent with the rigid and brittle nature of the gelatin network and the design principle of DN hydrogels. Consistently, gelatin/pHEAA DN gels exhibited extremely high tearing energy (i.e., high toughness), which monotonically increased from 974 to 5030 J/m² as the increase of gelatin concentrations (Figure 5a2). Such high tearing energy of fully physical gelatin/pHEAA DN gel was much higher than that of chemically cross-linked DN hydrogels, rubbers, and cartilages $(\sim 1000 \text{ J/m}^2).^{69-71}$

Second, in the case of pHEAA effect, gelatin/pHEAA hydrogels increased tensile stress from 0.74 to 2.33 MPa, elastic modulus from 0.12 to 4.32 MPa (Figure 5b1), and tearing energy from 1356 to 7783 J/m² (Figure 5b2) with the increase of pHEAA concentrations. Differently, there existed an optimal value of HEAA concentration of 40 wt % to achieve the largest tensile strain of 9.05. Since polyHEAA is softer and more ductile, the increase of HEAA concentration would construct the more densely and overlinked pHEAA network to strongly resist network deformation, as evidenced by the increase of tensile stress and elastic modulus at the expense of tensile strains.⁷² Moreover, the high HEAA concentration of >60 wt % also significantly reduced the water content of gelatin/pHEAA hydrogels to <30 wt %, making the gel display a plasticlike behavior. Taken together, after the network concentration effects are tested, gelatin/pHEAA hydrogel can achieve high mechanical strength of 1.93 MPa and bulk toughness of 4584 J/m² at optimal concentrations of gelation (10 wt %) and HEAA (50 wt %). Unless otherwise stated, we will use this optimal G₁₀H₅₀ gelatin/pHEAA DN hydrogel for the following tests.

Due to the presence of many hydrophilic groups (e.g., -OH, -NH₂, -COO⁻) in both gelatin and pHEAA networks, we hypothesize that gelatin/pHEAA DN gel is largely cross-linked by hydrogen bonds, which are considered as major contributors to enhancement of mechanical properties of the gels. To test this hypothesis, we selected and used two hydrogen-bond-breaking (HBB) agents (i.e., urea and NaSCN) to break hydrogen-bonding networks in the three as-prepared hydrogels (i.e., gelatin, pHEAA, and gelatin/ pHEAA hydrogels) and to examine the HBB impact on their mechanical properties. As shown in Figure 6a, the as-prepared gelatin and pHEAA SN hydrogels were transparent, while gelatin/pHEAA DN gels appeared milky white. Upon soaking the three gels in water, urea (5 M), and NaSCN (5 M) solutions at room temperature for 12 h, the three hydrogels underwent obvious swelling behaviors in all three solutions to different extents. Specifically, different swollen gelatin gel in water and gelatin gels in both urea and NaSCN solutions were dissolved, indicating that urea and NaSCN completely destroy a hydrogen-bonding network of gelatin SN hydrogel. Differently, while both pHEAA SN gel and gelatin/pHEAA DN gel swelled significantly in the three solutions by 2-2.2 times, NaSCN-induced partial disolvation of both hydrogels was still observed. In addition, swollen gelatin/pHEAA DN gel changed its appearance from milky to transparent. In addition, we also conducted swelling kinetics of gelatin/pHEAA DN gel in urea, NaSCN, and water. As shown in Figure 6b, gelatin/pHEAA in all solutions experienced a rapid swelling within the first 1 h, followed by reduced swelling rate to achieve the highest swelling ratio plateau of 12.99 in urea, 14.54 in NaSCN, and 8.67 in water after 12 h, respectively. As expected, considering urea and NaSCN are typical hydrogen-bond-breaking agents, gelatin/pHEAA underwent much higher swelling behaviors in urea and NaSCN solution than in water solution due to the loss of hydrogen bonds in hydrogels that in turn induces mechanical reduction and thus highlights the importance of hydrogen bonds in enhancing network interactions and maintain network structures. Furthermore, we examined the tensile stress/strain of the swollen gelatin/pHEAA DN gels in three solutions, and the results are summarized in Figure 6c. As expected, all swollen DN hydrogels were mechanically weak. The resultant tensile stress/strain of the swollen DN gels was

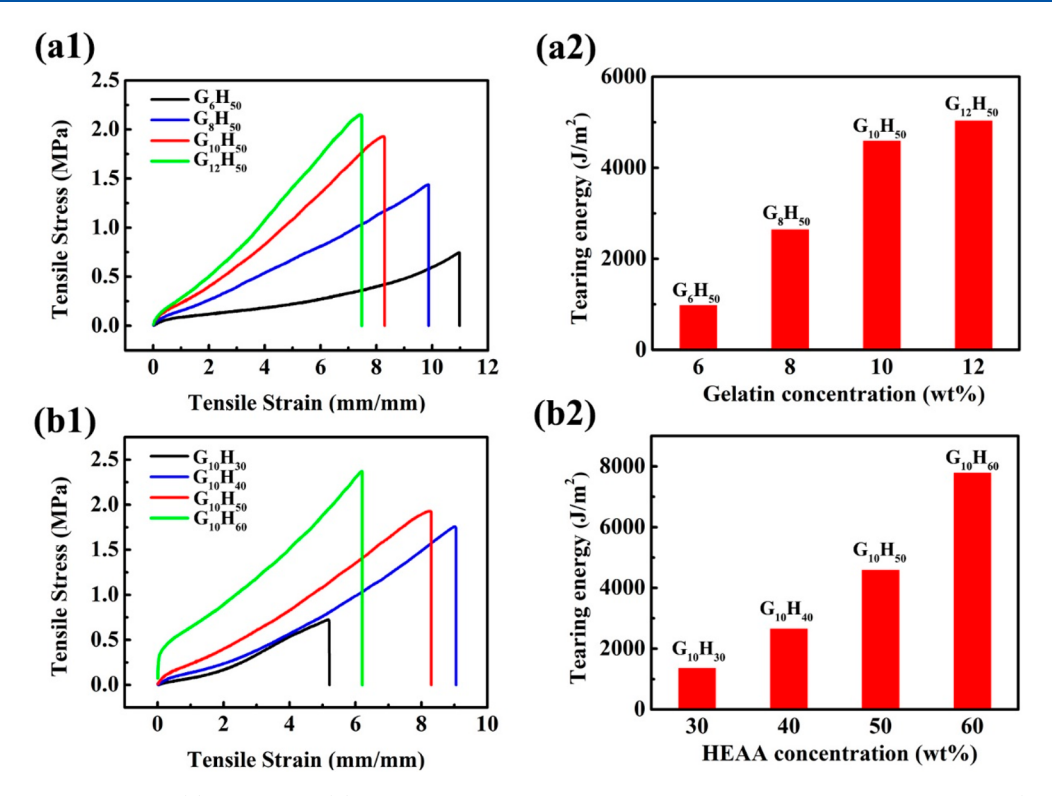


Figure 5. Concentration effects of (a) gelatin and (b) HEAA on mechanical properties of gelatin/pHEAA DN hydrogels by (a1, b1) tensile and (a2, b2) tearing tests. Gelatin/pHEAA DN hydrogels are prepared at (a) different gelatin concentrations of 6–12 wt % and a constant HEAA concentration of 50 wt % and (b) different HEAA concentrations of 30–60 wt % and a constant gelatin concentration of 10 wt %.

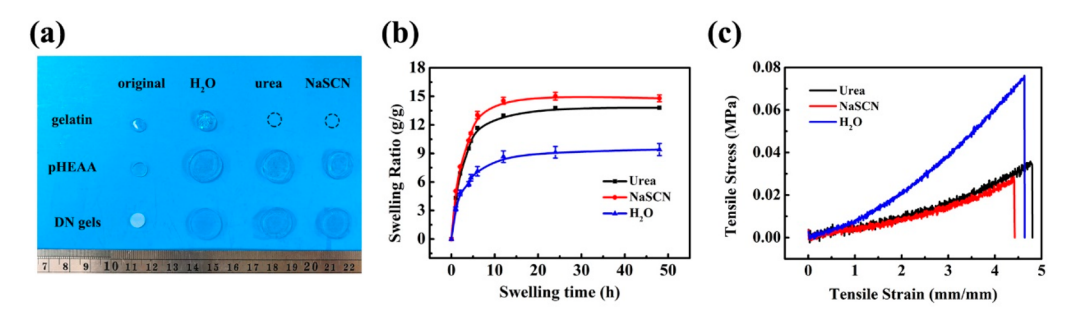


Figure 6. Swelling-induced mechanical reduction for hydrogels. (a) Photographs to describe the swelling behavior of gelatin SN, pHEAA SN, and $G_{10}H_{50}$ gelatin/pHEAA DN gels before and after soaking into water, urea (5 M), and NaSCN (5 M) solutions for 12 h. (b) Swelling kinetics of gelatin/pHEAA DN gel in water, urea (5 M), and NaSCN (5 M) solutions. (c) Tensile stress—strain curves of swollen gelatin/pHEAA DN gels after soaking into water, urea (5 M), and NaSCN (5 M) solutions for 12 h.

0.076 MPa/4.63 in water, 0.028 MPa/4.41 in NaSCN, and 0.036 MPa/4.78 in urea, as compared to 1.93 MPa/8.22 for asprepared DN hydrogel. Clearly, NaSCN and urea indeed destroy hydrogen bonds to reduce the mechanical properties of gelatin/pHEAA hydrogels, further confirming the important role of hydrogen bonds in mechanical enhancement of gelatin/pHEAA DN hydrogel.

Hysteresis, Softening, and Energy Dissipation of Gelatin/pHEAA DN Gels. We conducted different loading—unloading tests to better understand the energy dissipation mode of gelatin/pHEAA DN gels, another indicator of mechanical properties of the hydrogels. First, we tested the tensile properties of different fresh hydrogels to be stretched at different strains. In Figure 7a, all gelatin/pHEAA DN gels showed obvious hysteresis loops at different strains, and hysteresis loops gradually increased as strain (λ). Consequently, dissipated energies were very small as evidenced by

0.04 MJ/m³ at $\lambda = 1$ and 0.46 MJ/m³ at $\lambda = 3$ but increased rapidly to 1.64 MJ/m³ at $\lambda = 5$ and 3.67 MJ/m³ at $\lambda = 7$ (Figure 7b).

Furthermore, successive loading—unloading tests were also performed on the same hydrogel (Figure 7c) to examine their corresponding energy dissipation (Figure 7d). During the successive hysteresis loading—unloading test, no resting time occurred between any two consecutive loading cycles. Gelatin/pHEAA DN gel withstood five loading—unloading cycles as strain increased from 1 to 5 but was broken at the sixth cycle. Clearly, hysteresis loop increased its area as strains, and accordingly dissipated energy increased from 0.04 to 0.85 MJ/m³ (Figure 7d), but elastic modulus decreased from 0.52 to 0.26 MPa. Meanwhile, each reloading curve of a DN gel was close to but not completely overlapping the previous unloading curve, indicating that physical bonds in both networks that broke during the loading cycle were partially restored from its

Macromolecules

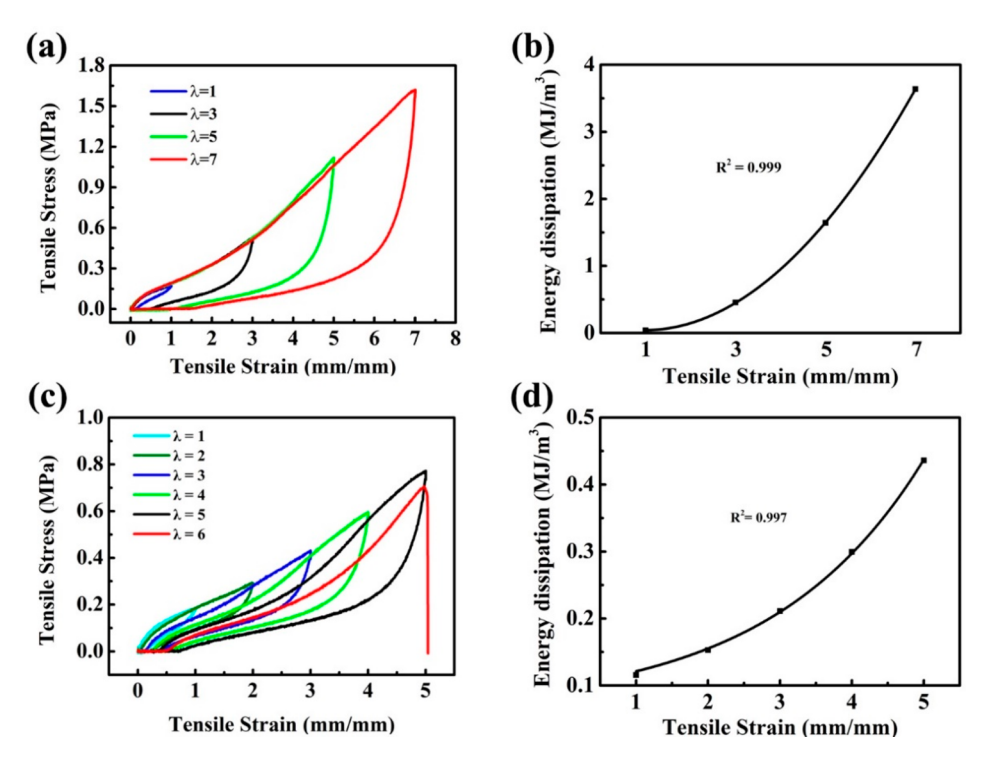


Figure 7. (a) Cyclic loading—unloading curves and (b) the corresponding dissipated energies of different $G_{10}H_{50}$ gelatin/pHEAA DN hydrogels at different strains. (c) Successive hysteresis loading—unloading curves and (d) the corresponding dissipated energies of the same $G_{10}H_{50}$ gelatin/pHEAA DN hydrogels at different strains.

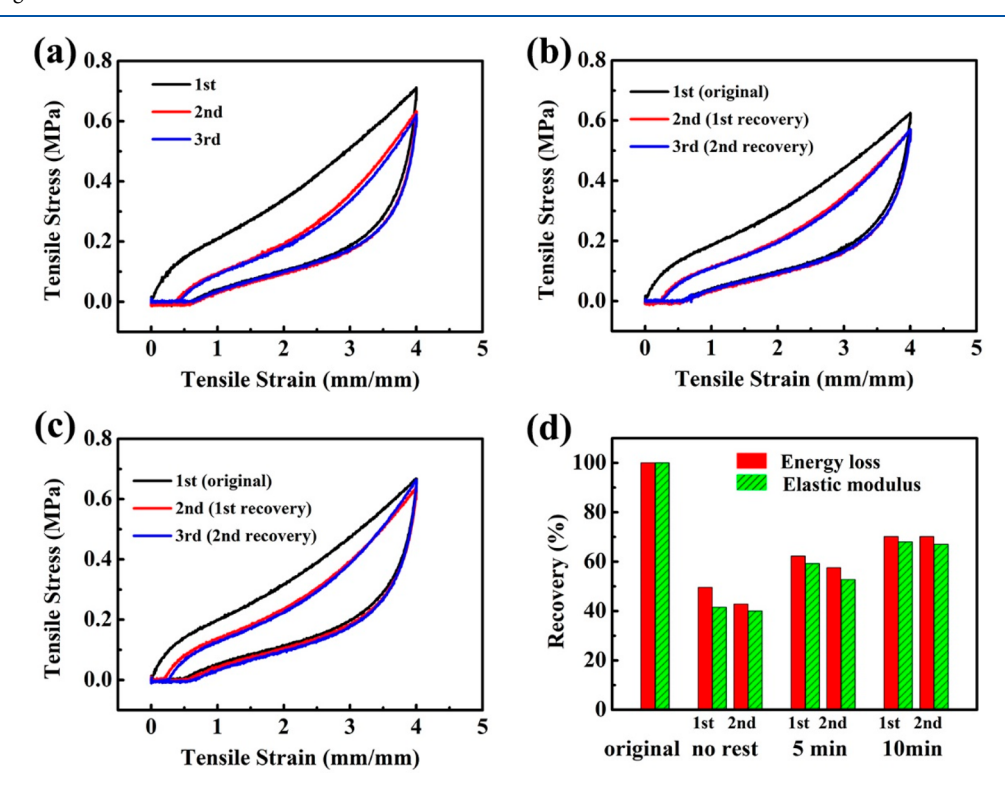


Figure 8. Self-recovery of $G_{10}H_{50}$ gelatin/pHEAA hydrogels using three successive loading—unloading tests at a strain of 4, room temperature, and different resting times between two cycles of (a) 0, (b) 5, and (c) 10 min. (d) Quantitative analysis of toughness (energy loss) and stiffness (elastic modulus) recovery ratios, calculated from stress–strain curves from (a)–(c).

immediate unloading cycle. When the original stress—strain curve in Figure 7a was compared with the successive loading—unloading stress—strain curve in Figure 7c, the original hydrogels always had a higher stress than the loading—

unloading hydrogels at the same strain. This implies that during the (re)loading process, the second pHEAA network also helps to bear stress and dissipate energy as the first gelatin network is fractured, thus leading to high mechanical strength

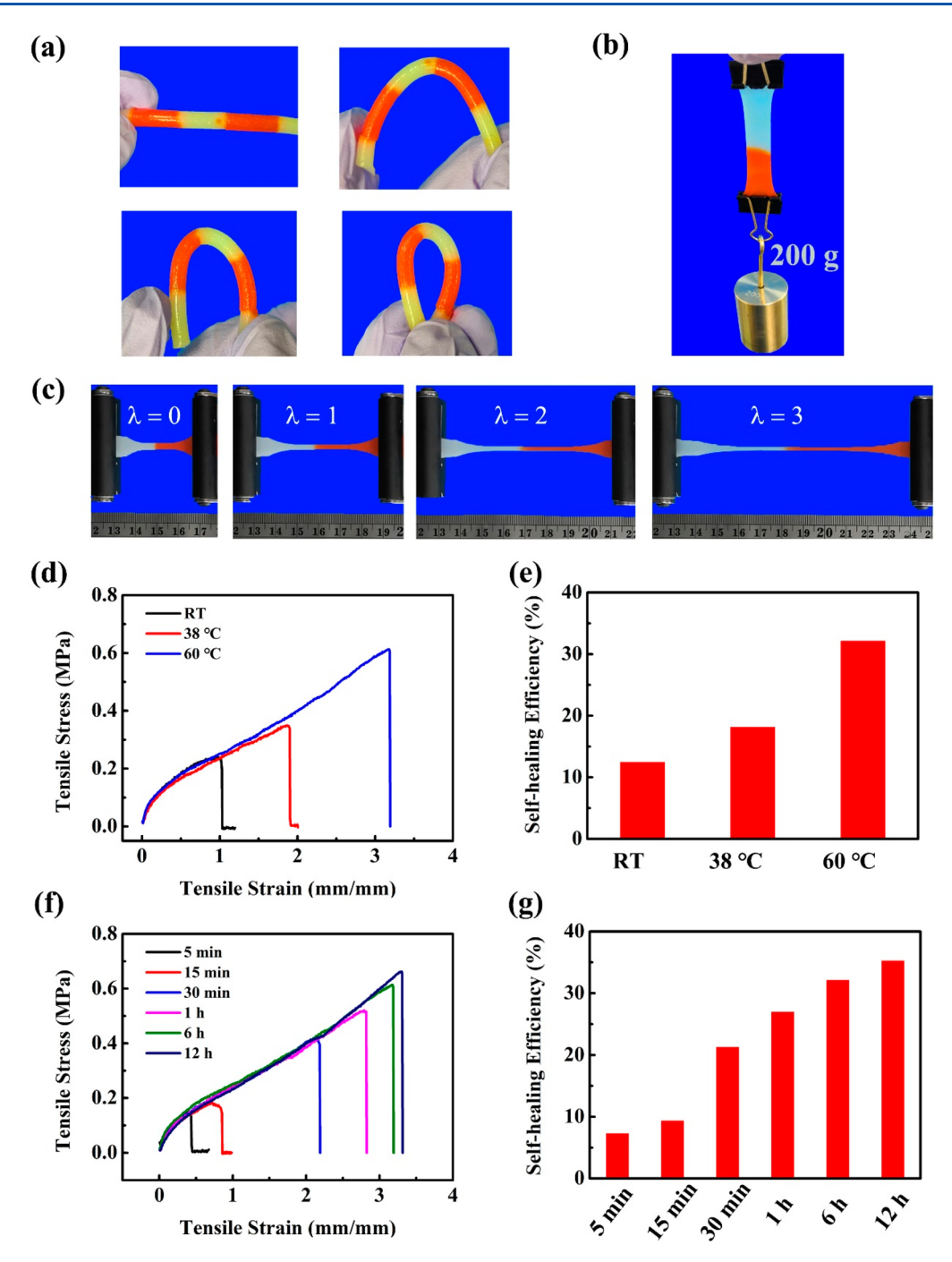


Figure 9. Self-healing properties of $G_{10}H_{50}$ gelatin/pHEAA DN hydrogels. Self-healed gelatin/pHEAA hydrogels withstand (a) multiple, intensive bending toward different angles, (b) a weight lifting of 200 g, and (c) a stretching from 1 to 3 times of its original length. Tensile properties and self-healing efficiency of self-healed gelatin/pHEAA hydrogels at (d)–(e) different heating treatments for 6 h and (f)–(g) different heating times at $60\,^{\circ}C$

and toughness in DN gels.²⁵ Also, the large energy dissipation stems from (i) the breakage of reversible hydrogen bond between inter- and intranetworks and (ii) the pulling out of gelatin chains from gelatin helical bundles.

Self-Recovery and Self-Healing Properties of Gelatin/pHEAA DN Gels. Due to the reversible nature of network interactions in gelatin/pHEAA hydrogels, we also used the three loading—unloading cycles to examine the mechanical self-recovery of gelatin/pHEAA hydrogels at a strain of 4 as a function of resting times (i.e., 0, 5, and 10 min) between two adjacent cycles. As a control without any resting between two

cycles, Figure 8a shows that gelatin/pHEAA hydrogel displayed a large hysteresis loop (i.e., dissipated a large energy of 0.90 MJ/m³) in the first loading—unloading cycle. The hysteresis loop was reduced by ~50% in the immediate second loading—unloading cycle and remained almost unchanged in the third loading—unloading cycle. This indicates that after the softening occurs in the first cycle, the fractured networks cannot be recovered immediately without any resting at room temperature. On the other hand, such network fracture did not become worse due to the existence of unbroken physical interactions. By increasing different resting times of 5 or 10

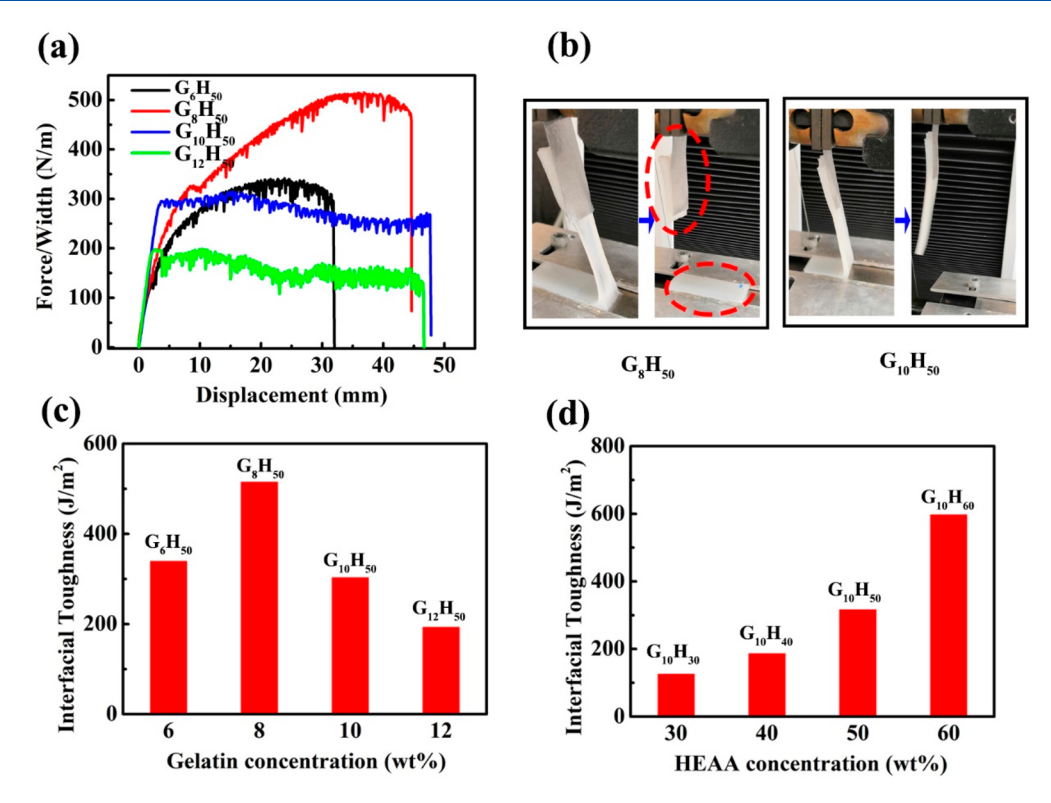


Figure 10. Interfacial toughness of gelatin/pHEAA DN hydrogel on titanium (Ti) substrate. (a) Typical peeling force/width curves of different composition gelatin/pHEAA DN hydrogels as a function of gelatin concentrations at a peeling rate of 50 mm/min. (b) Peeling process of G_8H_{50} and $G_{10}H_{50}$ gelatin/pHEAA DN hydrogels from Ti substrate. Interfacial toughness of gelatin/pHEAA DN hydrogels on Ti substrate as a function of (c) gelatin and (d) HEAA concentrations.

min after each unloading cycle, the changes of hysteresis loops (i.e., hysteresis energy) followed the same trend (Figure 8bc); i.e., hysteresis energy was reduced after the first cycle and remained almost unchanged in the following cycles. Meanwhile, visual inspection also showed that the increase of resting time also helps to recover the networks to a larger extent. Quantitatively, we further examined both elastic modulusbased (stiffness) self-recovery and dissipated energy-based (toughness) self-recovery of gelatin/pHEAA DN gels in response to resting time after the first loading-unloading. In Figure 8d, gelatin/pHEAA gels recovered their toughness/ stiffness to 49.5%/41.5%, 62.3%/59.3%, and 70.2%/68.0% in the first cycle and 42.9/40.0%, 57.6%/52.8%, and 70.2%/ 67.0% in the second cycle after 0, 5, and 10 min resting at room temperature, respectively. Clearly, toughness/stiffness recovery rates increased as resting time, suggesting that the internal damage of networks can be much better recovered with the increase of resting time before reloading. On the other hand, increase of resting time from 5 to 10 min only slightly improves toughness/stiffness by 8-9%, indicating that the repair of hydrogen bonds in the networks could occur within 5 min, and such rapid self-recovery property of gelatin/pHEAA DN gel also indicates good fatigue resistance of the gel at the

We further challenged the self-healing property of gelatin/pHEAA DN gels. The gelatin/pHEAA DN gels were first cut into two or multiple pieces completely, and then the separated gel pieces were physically put together without applying any external force. Due to a thermoreversible sol—gel property of gelatin, we applied the heat to the physically attached gel to promote the self-healing property. At first glance, the four-cut gelatin/pHEAA gels can be self-healed into a single gel with

alternative red and yellow colors at 60 °C for 6 h. The healed gel can withstand the extensive bending back-and-forth by multiple times (Figure 9a), a weight lifting of 200 g (Figure 9b), and a stretching up to 3 times of original length (Figure 9c).

Quantitatively, we investigated the mechanical properties of the healed gelatin/pHEAA DN gels as a function of heating temperatures and heating times. Figure 9d shows that as a control, without the heating treatment, self-healed gel at room temperature (RT) exhibited very weak tensile stress of 0.24 MPa at a fracture strain of 1. Upon the heating treatment of healed gels at a physiological temperature of 38 °C for 6 h, fracture tensile stress and strain increased to 0.35 MPa and 1.9, respectively. Further increase of heating temperature to 60 °C continuously increased the tensile stress/strain to 0.62 MPa/ 3.20, which was 2-3 times higher than those of heatinguntreated gels. Figure 9e showed that the self-healing efficiency of gelatin/pHEAA DN gels increased from 12.4% at 25 °C, 18.1% at 38 °C, to 32.1% at 60 °C. At room temperature, the self-healing capacity of gelatin/pHEAA gels mainly results from the self-association of the second pHEAA network via hydrogen bonds.¹⁸ On the other hand, considering that heating-induced gelatin structural conversion between random coils at the higher temperatures during the heating process and helical bundles at the lower temperatures during the cooling process is a reversible process, the self-healing properties of heat-treated gelatin/pHEAA gels mainly originate from multiple, reversible physical interactions of hydrogen bonds and van der Waals interactions between and within both networks, differing from that of heat-untreated gels. To further test the above-mentioned explanation, we examined the effect of heating time on the tensile properties (Figure 9f) and self-

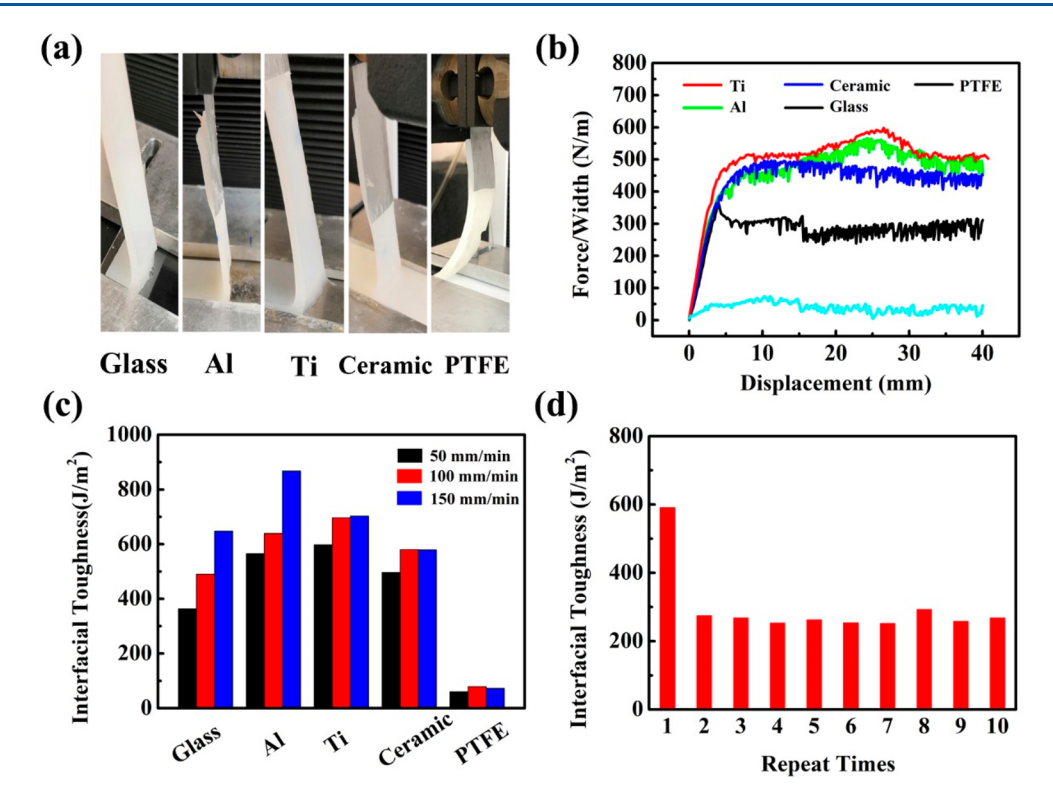


Figure 11. Interfacial toughness of $G_{10}H_{60}$ gelatin/pHEAA hydrogels on different solid substrates. (a) Peeling process and (b) peeling force/width curves of gelatin/pHEAA gels from glass, Al, Ti, ceramic, and PTFE substrates at a peeling rate of 50 mm/min. (c) Effect of peeling rates on the interfacial toughness of gelatin/pHEAA hydrogels on glass, Al, Ti, ceramic, and PTFE substrates. (d) Reversible interfacial toughness of $G_{10}H_{60}$ gelatin/pHEAA hydrogels by 10 times adhesion on/peel off cycles on Ti at a peeling rate of 50 mm/min.

healing efficiency (Figure 9g) of gelatin/pHEAA DN gels at 60 °C. Due to thermoresponsive nature of gelatin, the increase of heating time at 60 °C from 5 min to 12 h improved the tensile stress/strain/self-healing efficiency of self-healed gels from 0.14 MPa/0.43/7.25% at 5 min, 0.18 MPa/0.74/9.33% at 15 min, 0.41 MPa/2.18/21.24% at 30 min, 0.52 MPa/2.81/26.94% at 1 h, 0.62 MPa/3.20/32.12% at 6 h, to 0.68 MPa/3.30/35.23% at 12 h, respectively. This indicates that increase of heating time allows the reassociation of the gelatin helical bundles together in a more efficient way. The degree of mechanical improvement became less pronounced when heating times were prolonged. Taken together, high self-recovery as resting time and self-healing as heating temperature/time indicate that both networks reversibly break and reform to repair network damage via physical bonds (hydrogen bonds, chain conformational changes, and van der Waals interactions).

Interfacial Toughness of Gelatin/pHEAA DN Gels. Adhesive hydrogels on different surfaces have an increasing impact on many potential applications including wound dressings, tissue engineering, wearable devices, and human—machine interfaces. Generally speaking, adhesive hydrogels require high interfacial toughness to maintain the gel—surface interface for achieving their functions, where interfacial toughness is attributed to two main factors of high bulk toughness and strong gel—surface bindings. In this work, upon demonstrating high mechanical and self-recovery/healing properties of gelatin/pHEAA DN gels, we aim to test whether the gelatin/pHEAA gels also possess high surface adhesive capacity (i.e., high interfacial toughness).

First, we examined the effect of two network concentrations on the interfacial toughness of gelatin/pHEAA DN gels on titanium (Ti) using the 90° peeling test. There was no surface

modification on Ti substrate for promoting the interfacial bonding between the gel and Ti substrate. The 90° peeling test in Figure 10a shows the force/width-displacement curves of gelatin/pHEAA DN gels. Without any surface modification, gelatin/pHEAA hydrogels made of the lower gelatin concentration (6 or 8 wt %) appeared to show a higher intensity of force/width than the gels of the higher gelatin concentration (10 or 12 wt %). Based on the forcedisplacement curves, interfacial toughness of gelatin/pHEAA DN gels was estimated to be \sim 339, \sim 515, \sim 303, and \sim 193 J/ m² at 6, 8, 10, and 12 wt % of gelatin, respectively (Figure 10c). On the other hand, it was also observed that the hydrogels of the lower gelatin concentrations did not achieve a relative stable force plateau, indicating that bulk hydrogels are broken before completely peeling off from the Ti substrate. Visual inspection in Figure 10b confirmed that while both gelatin/pHEAA DN hydrogels made of 8% or 10% gelatin can be easily attached onto the Ti surface, the 8% gelatin/pHEAA hydrogel cannot be completely peeled off from the Ti substrate because it cracked in bulk phase prior to peeling off, while the 10 wt % gelatin/pHEAA hydrogel can be easily peeled off from Ti substrate due to its weak surface adhesion and strong bulk toughness. Second, in the case of HEAA concentration effect, Figure 10d showed that interfacial toughness of gelatin/ pHEAA gels increased from 125 to 597 J/m² as HEAA concentration increased from 30 to 60 wt %, consistent with the increase of bulk toughness as HEAA concentration, indicating that strong hydrogel-solid interface generally requires high fracture toughness of the hydrogel itself to ensure that the adhesion failure occurs at the gel-solid interface, not in the body of the gel.

Second, we further tested whether gelatin/pHEAA DN gels possess a general surface adhesion property to adhere on different solid substrates including aluminum (Al), ceramic, glass, and poly(tetrafluoroethylene) (PTFE). As shown in Figure 11a, gelatin/pHEAA hydrogels can easily adhere on and peel off from different solid substrates. Quantitatively, Figure 11b shows the peeling-force-displacement curves of DN gels on different substrates at a peeling rate of 50 mm/min. Gelatin/pHEAA gels exhibited strong adhesion on hydrophilic substrates (Ti, Al, ceramic, and glass) with peeling forces of $364-597 \text{ J/m}^2 (\text{J/m}^2 = \text{N/m})$ but extremely weak adhesion on hydrophobic substrate (PTFE) with very low peeling force of 60 J/m². These results, from another viewpoint, confirm that strong interfacial binding between gelatin/pHEAA DN gels and hydrophilic solid substrates mainly stems from hydrogen bonds, while hydrophobic PTFE surface cannot form massive hydrogen bonds with the gels, thus leading to weak interfacial toughness.

Third, we further studied the effect of peeling rate on the interfacial toughness of gelatin/pHEAA DN gels on different solid substrates. Figure 11c shows that for all hydrophilic substrates, interfacial toughness of the hydrogels increased as peeling rates; i.e., the measured interfacial toughness was 364 \rightarrow 490 \rightarrow 645 J/m² on glass, 565 \rightarrow 639 \rightarrow 867 J/m² on Al, $597 \rightarrow 696 \rightarrow 702 \text{ J/m}^2 \text{ on Ti, and } 496 \rightarrow 579 \rightarrow 579 \text{ J/m}^2$ on ceramics as peeling rate increased from $50 \rightarrow 100 \rightarrow 150$ mm/min. It appeared that Al and Ti had relatively higher interfacial toughness than glass and ceramic, presumably because Al and Ti substrates contain oxide-rich groups to interact with hydrophilic hydroxyl, amide, and amino groups of the gels, which helps to produce the stronger interfacial force between hydrogel and substrate via hydrogen bonding, metal complexation, and van der Waal interactions. The rate dependence on interfacial toughness on hydrophilic substrates also explains the viscoelasticity of the gelatin/pHEAA DN gels, which are correlated with the rate-dependent energy dissipation behavior. In contrast, the gels had very weak interfacial toughness on hydrophobic PTFE surface (60-78-72 J/m^2), almost independent of peeling rates.

Finally, we investigated the reversible adhesive property of gelatin/pHEAA hydrogels on Ti, one of the strongest gelsolid systems in this work. We repeatedly adhered the gel on and peeled the gel off of Ti substrate10 times, with 5 min resting time between two adhere on/peeling off actions. Figure 11d shows the reduction of interfacial toughness from 600 J/ m² at the first peeling off test to 300 J/m² at the second and thereafter peeling off tests. Clearly, initial polymerization of gelatin/pHEAA on Ti substrate allows formation of sufficient interfacial bonds between gel and Ti and also the repeling of all potential bubbles at gel/Ti interface; thus, both effects empower the gel to tightly adhere on the surface, leading to high interfacial toughness of 600 J/m². But, after the first the peeling off, some small fractured gel residues may still stick to the surface, which causes the inevitable bubble formation between re-adhered gel and surface and reduces their interfacial interactions on a relatively rough and modified surface. Also, the re-adhering of the gel on the surface requires much longer time to re-establish some strong interfacial bonds. Thus, not all interfacial bonds can be recovered. On the other hand, some weak and reversible physical bonds (e.g., van der Waals interactions) at the gel/Ti interface can always form instantly almost independent of peeling times, explaining the

almost unchanged interfacial toughness of \sim 250 J/m² after multiple peeling off tests.

To better understand the mechanical toughening and recovery mechanisms of gelatin/pHEAA DN gel, we purposely compare structure and mechanical properties between two similar gelatin/pHEAA gel and agar/pHEAA DN gel, 18 both of which share the same second network of pHEAA and a similar first network (gelatin vs agar) with sol-gel-trigger random-tohelix structural transition. Some similarities and differences between the two hydrogels were observed. From a different structural/property viewpoint, agar/pHEAA DN gel and gelatin/pHEAA DN gel have a different gelation temperature due to different sol-gel temperatures of agar ($T_{\rm m} = 85-95$ °C) and gelatin ($T_{\rm m}$ = 26–30 °C). Thus, gelatin/pHEAA DN gel can be self-recovered at relatively low temperatures (even at room temperature or physiological temperature), making them more appropriate for biorelated applications at physiological conditions. Also, agar molecules containing a large amount of -OH and possessing unique six-membered ringlike structure allow construction of a highly dense hydrogen-bonding network as compared to gelatin molecules, so agar/pHEAA DN gel (tensile strength of 2.6 MPa and tearing energy of 7896 J/m²) possesses a stronger strength than gelatin/pHEAA DN gel (tensile strength of 1.93 MPa and tearing energy of 4584 J/ m²). On the other hand, from a similar viewpoint, since both gelatin and agar undergo the structural transition from random coils to helical bundles during the cooling down sol-to-gel process, when forces are applied to the gels, helical bundles of gelatin or agar start to separate from each other, followed by the breaking of hydrogen bonds to disassociate gelatin or agar from helical bundles, contributing to energy dissipation. So, during the deformation process, both agar/pHEAA and gelatin/pHEAA DN gels exhibited simultaneous necking and yielding phenomenon, probably indicating that the first network retains its continuous phase while still intertwining with the second network.

CONCLUSIONS

In this work, we have designed and fabricated a fully physically linked gelatin/pHEAA DN hydrogel, consisting of the first gelatin network and the second pHEAA network. Since no chemical cross-linker was introduced into the gelatin/pHEAA hydrogel system, both networks were gelated by hydrogen bonds. The resultant gelatin/pHEAA DN hydrogels exhibited multiple superior mechanical properties, including high strength (tensile stress of 1.93 MPa), extensibility (tensile strain of 8.2), stiffness (0.52 MPa), and toughness (tearing energy of 4584 J/m²), fast toughness/stiffness recovery of 70.2%/68.0%, good self-healed tensile stress/strain of 0.62 MPa/3.2, strong interfacial toughness of 579-867 J/m² on different solid surfaces, and repeatable interfacial toughness of \sim 250 J/m². Further comparison of the two similar physical DN hydrogels between gelatin/pHEAA and agar/pHEAA revealed some similarity and difference in toughening, recovery, and adhesive properties, suggesting a "chain pulling-out" mechanism to dissipate energy and toughen hydrogels. A unique combination of topological DN structure and reversible network interactions synergistically improves the mechanical properties of the hydrogels in bulk and on solid surfaces. This double-network physical cross-linking design strategy could be applied to other polymer, elastomer, or hydrogel systems with comparable or even better mechanical properties as compared to those chemically cross-linked systems.

ASSOCIATED CONTENT

Supporting Information

The Supporting Information is available free of charge at https://pubs.acs.org/doi/10.1021/acs.macromol.9b01686.

Abbreviation of hybrid chemically—physically cross-linked and fully physically cross-linked DN hydrogels (Table S1) (PDF)

AUTHOR INFORMATION

Corresponding Authors

*E-mail: jxtang0733@163.com (J.T.). *E-mail: zhengj@uakron.edu (J.Z.).

ORCID ®

Yung Chang: 0000-0003-1419-4478 Jie Zheng: 0000-0003-1547-3612

Author Contributions

 $^{\perp}$ These authors contributed equally to this work.

Notes

The authors declare no competing financial interest.

ACKNOWLEDGMENTS

J.Z. acknowledges financial support from NSF (CMMI-1825122). J.T. acknowledges financial support from the National Natural Scientific Foundation of China (51774128).

REFERENCES

- (1) Zheng, W. J.; An, N.; Yang, J. H.; Zhou, J.; Chen, Y. M. Tough Al-alginate/poly(N-isopropylacrylamide) hydrogel with tunable LCST for soft robotics. ACS Appl. Mater. Interfaces 2015, 7 (3), 1758–64.
- (2) Yuk, H.; Lin, S.; Ma, C.; Takaffoli, M.; Fang, N. X.; Zhao, X. Hydraulic hydrogel actuators and robots optically and sonically camouflaged in water. *Nat. Commun.* **2017**, *8*, 14230.
- (3) Xiao, S.; Zhang, M.; He, X.; Huang, L.; Zhang, Y.; Ren, B.; Zhong, M.; Chang, Y.; Yang, J.; Zheng, J. Dual Salt- and Thermo-Responsive Programmable Bilayer Hydrogel Actuators with Pseudo-Interpenetrating Double-Network Structures. ACS Appl. Mater. Interfaces 2018, 10, 21642.
- (4) Liao, M.; Wan, P.; Wen, J.; Gong, M.; Wu, X.; Wang, Y.; Shi, R.; Zhang, L. Wearable, Healable, and Adhesive Epidermal Sensors Assembled from Mussel-Inspired Conductive Hybrid Hydrogel Framework. *Adv. Funct. Mater.* **2017**, 27 (48), 1703852.
- (5) Tai, Y.; Mulle, M.; Aguilar Ventura, I.; Lubineau, G. A highly sensitive, low-cost, wearable pressure sensor based on conductive hydrogel spheres. *Nanoscale* **2015**, *7* (35), 14766–73.
- (6) Cai, G.; Wang, J.; Qian, K.; Chen, J.; Li, S.; Lee, P. S. Extremely Stretchable Strain Sensors Based on Conductive Self-Healing Dynamic Cross-Links Hydrogels for Human-Motion Detection. *Adv. Sci.* (Weinh) **2017**, 4 (2), 1600190.
- (7) Singh, Y. P.; Bhardwaj, N.; Mandal, B. B. Potential of Agarose/Silk Fibroin Blended Hydrogel for in Vitro Cartilage Tissue Engineering. ACS Appl. Mater. Interfaces 2016, 8 (33), 21236–49.
- (8) Liu, M.; Zeng, X.; Ma, C.; Yi, H.; Ali, Z.; Mou, X.; Li, S.; Deng, Y.; He, N. Injectable hydrogels for cartilage and bone tissue engineering. *Bone Res.* **2017**, *5*, 17014.
- (9) Ren, K.; He, C.; Xiao, C.; Li, G.; Chen, X. Injectable glycopolypeptide hydrogels as biomimetic scaffolds for cartilage tissue engineering. *Biomaterials* **2015**, *51*, 238–249.
- (10) Pan, C.; Liu, L.; Chen, Q.; Zhang, Q.; Guo, G. Tough, Stretchable, Compressive Novel Polymer/Graphene Oxide Nanocomposite Hydrogels with Excellent Self-Healing Performance. ACS Appl. Mater. Interfaces 2017, 9 (43), 38052–38061.
- (11) Haraguchi, K.; Takehisa, T. Nanocomposite Hydrogels: A Unique Organic-Inorganic Network Structure with Extraordinary

Mechanical, Optical, and Swelling/De-swelling Properties. *Adv. Mater.* **2002**, *14* (16), 1120–1124.

- (12) Shin, M. K.; Spinks, G. M.; Shin, S. R.; Kim, S. I.; Kim, S. J. Nanocomposite Hydrogel with High Toughness for Bioactuators. *Adv. Mater.* **2009**, *21* (17), 1712–1715.
- (13) Li, J.; Illeperuma, W. R. K.; Suo, Z.; Vlassak, J. J. Hybrid Hydrogels with Extremely High Stiffness and Toughness. *ACS Macro Lett.* **2014**, 3 (6), 520–523.
- (14) He, X.; Zhang, C.; Wang, M.; Zhang, Y.; Liu, L.; Yang, W. An Electrically and Mechanically Autonomic Self-healing Hybrid Hydrogel with Tough and Thermoplastic Properties. *ACS Appl. Mater. Interfaces* **2017**, *9* (12), 11134–11143.
- (15) Chen, Q.; Zhu, L.; Zhao, C.; Wang, Q.; Zheng, J. A robust, one-pot synthesis of highly mechanical and recoverable double network hydrogels using thermoreversible sol-gel polysaccharide. *Adv. Mater.* **2013**, 25 (30), 4171–6.
- (16) Gong, J. P.; Katsuyama, Y.; Kurokawa, T.; Osada, Y. Doublenetwork hydrogels with extremely high mechanical strength. *Adv. Mater.* **2003**, *15* (14), 1155–1158.
- (17) Gong, J. P. Why are double network hydrogels so tough? *Soft Matter* **2010**, *6* (12), 2583.
- (18) Chen, H.; Liu, Y.; Ren, B.; Zhang, Y.; Ma, J.; Xu, L.; Chen, Q.; Zheng, J. Super Bulk and Interfacial Toughness of Physically Crosslinked Double-Network Hydrogels. *Adv. Funct. Mater.* **2017**, 27 (44), 1703086.
- (19) Zhang, Y.; Ren, B.; Xie, S.; Cai, Y.; Wang, T.; Feng, Z.; Tang, J.; Chen, Q.; Xu, J.; Xu, L.; Zheng, J. Multiple Physical Cross-Linker Strategy To Achieve Mechanically Tough and Reversible Properties of Double-Network Hydrogels in Bulk and on Surfaces. ACS Applied Polymer Materials 2019, 1, 701.
- (20) Deng, Y.; Huang, M.; Sun, D.; Hou, Y.; Li, Y.; Dong, T.; Wang, X.; Zhang, L.; Yang, W. Dual Physically Cross-Linked kappa-Carrageenan-Based Double Network Hydrogels with Superior Self-Healing Performance for Biomedical Application. *ACS Appl. Mater. Interfaces* **2018**, *10* (43), 37544–37554.
- (21) Yuan, N.; Xu, L.; Wang, H.; Fu, Y.; Zhang, Z.; Liu, L.; Wang, C.; Zhao, J.; Rong, J. Dual Physically Cross-Linked Double Network Hydrogels with High Mechanical Strength, Fatigue Resistance, Notch-Insensitivity, and Self-Healing Properties. *ACS Appl. Mater. Interfaces* **2016**, 8 (49), 34034–34044.
- (22) Li, X.; Zhang, Y.; Yang, Q.; Li, D.; Zhang, G.; Long, S. Agar/PAAc-Fe3+ hydrogels with pH-sensitivity and high toughness using dual physical cross-linking. *Iran. Polym. J.* **2018**, 27 (11), 829–840.
- (23) Sun, J. Y.; Zhao, X.; Illeperuma, W. R.; Chaudhuri, O.; Oh, K. H.; Mooney, D. J.; Vlassak, J. J.; Suo, Z. Highly stretchable and tough hydrogels. *Nature* **2012**, *489* (7414), 133–6.
- (24) Chen, H.; Yang, F.; Hu, R.; Zhang, M.; Ren, B.; Gong, X.; Ma, J.; Jiang, B.; Chen, Q.; Zheng, J. A comparative study of the mechanical properties of hybrid double-network hydrogels in swollen and as-prepared states. *J. Mater. Chem. B* **2016**, 4 (35), 5814–5824.
- (25) Yan, X.; Chen, Q.; Zhu, L.; Chen, H.; Wei, D.; Chen, F.; Tang, Z.; Yang, J.; Zheng, J. High strength and self-healable gelatin/polyacrylamide double network hydrogels. *J. Mater. Chem. B* **2017**, *S* (37), 7683–7691.
- (26) Tang, Z.; Chen, Q.; Chen, F.; Zhu, L.; Lu, S.; Ren, B.; Zhang, Y.; Yang, J.; Zheng, J. General Principle for Fabricating Natural Globular Protein-Based Double-Network Hydrogels with Integrated Highly Mechanical Properties and Surface Adhesion on Solid Surfaces. *Chem. Mater.* **2019**, *31* (1), 179–189.
- (27) Yang, Y.; Wang, X.; Yang, F.; Shen, H.; Wu, D. A Universal Soaking Strategy to Convert Composite Hydrogels into Extremely Tough and Rapidly Recoverable Double-Network Hydrogels. *Adv. Mater.* **2016**, 28 (33), 7178–7184.
- (28) Li, J.; Suo, Z.; Vlassak, J. J. Stiff, strong, and tough hydrogels with good chemical stability. *J. Mater. Chem. B* **2014**, 2 (39), 6708–6713.
- (29) Diao, W.; Wu, L.; Ma, X.; Zhuang, Z.; Li, S.; Bu, X.; Fang, Y. Highly stretchable, ionic conductive and self-recoverable zwitterionic polyelectrolyte-based hydrogels by introducing multiple supra-

molecular sacrificial bonds in double network. J. Appl. Polym. Sci. 2019, 136 (29), 47783.

- (30) Chen, F.; Chen, Q.; Zhu, L.; Tang, Z.; Li, Q.; Qin, G.; Yang, J.; Zhang, Y.; Ren, B.; Zheng, J. General strategy to fabricate strong and tough low-molecular-weight gelator-based supramolecular hydrogels with double network structure. *Chem. Mater.* **2018**, *30* (5), 1743–1754.
- (31) Lu, X.; Chan, C. Y.; Lee, K. I.; Ng, P. F.; Fei, B.; Xin, J. H.; Fu, J. Super-tough and thermo-healable hydrogel promising for shape-memory absorbent fiber. *J. Mater. Chem. B* **2014**, 2 (43), 7631–7638.
- (32) Liu, S.; Li, L. Recoverable and Self-Healing Double Network Hydrogel Based on kappa-Carrageenan. ACS Appl. Mater. Interfaces 2016, 8 (43), 29749–29758.
- (33) Niu, R.; Qin, Z.; Ji, F.; Xu, M.; Tian, X.; Li, J.; Yao, F. Hybrid pectin-Fe(3+)/polyacrylamide double network hydrogels with excellent strength, high stiffness, superior toughness and notchinsensitivity. *Soft Matter* **2017**, *13* (48), 9237–9245.
- (34) Chen, Q.; Yan, X.; Zhu, L.; Chen, H.; Jiang, B.; Wei, D.; Huang, L.; Yang, J.; Liu, B.; Zheng, J. Improvement of mechanical strength and fatigue resistance of double network hydrogels by ionic coordination interactions. *Chem. Mater.* **2016**, 28 (16), 5710–5720.
- (35) Chen, F.; Tang, Z.; Lu, S.; Zhu, L.; Wang, Q.; Gang, Q.; Yang, J.; Chen, Q. Fabrication and mechanical behaviors of novel supramolecular/polymer hybrid double network hydrogels. *Polymer* **2019**, *168*, 159–167.
- (36) Yang, Y.; Wang, X.; Yang, F.; Wang, L.; Wu, D. Highly Elastic and Ultratough Hybrid Ionic-Covalent Hydrogels with Tunable Structures and Mechanics. *Adv. Mater.* **2018**, *30* (18), No. e1707071.
- (37) Zhu, J.; Guan, S.; Hu, Q.; Gao, G.; Xu, K.; Wang, P. Tough and pH-sensitive hydroxypropyl guar gum/polyacrylamide hybrid doublenetwork hydrogel. *Chem. Eng. J.* **2016**, *306*, 953–960.
- (38) Wei, D.; Yang, J.; Zhu, L.; Chen, F.; Tang, Z.; Qin, G.; Chen, Q. Fully physical double network hydrogels with high strength, rapid self-recovery and self-healing performances. *Polym. Test.* **2018**, *69*, 167–174.
- (39) Wang, M. X.; Chen, Y. M.; Gao, Y.; Hu, C.; Hu, J.; Tan, L.; Yang, Z. Rapid Self-Recoverable Hydrogels with High Toughness and Excellent Conductivity. ACS Appl. Mater. Interfaces 2018, 10 (31), 26610—26617
- (40) Gong, Z.; Zhang, G.; Zeng, X.; Li, J.; Li, G.; Huang, W.; Sun, R.; Wong, C. High-Strength, Tough, Fatigue Resistant, and Self-Healing Hydrogel Based on Dual Physically Cross-Linked Network. ACS Appl. Mater. Interfaces 2016, 8 (36), 24030–7.
- (41) Jia, H.; Huang, Z.; Fei, Z.; Dyson, P. J.; Zheng, Z.; Wang, X. Unconventional Tough Double-Network Hydrogels with Rapid Mechanical Recovery, Self-Healing, and Self-Gluing Properties. *ACS Appl. Mater. Interfaces* **2016**, 8 (45), 31339–31347.
- (42) Chen, Q.; Zhu, L.; Chen, H.; Yan, H.; Huang, L.; Yang, J.; Zheng, J. A novel design strategy for fully physically linked double network hydrogels with tough, fatigue resistant, and self-healing properties. *Adv. Funct. Mater.* **2015**, 25 (10), 1598–1607.
- (43) Zhang, B.; Gao, Z.; Gao, G.; Zhao, W.; Li, J.; Ren, X. Highly Mechanical and Fatigue-Resistant Double Network Hydrogels by Dual Physically Hydrophobic Association and Ionic Crosslinking. *Macromol. Mater. Eng.* **2018**, 303 (7), 1800072.
- (44) Xia, S.; Song, S.; Gao, G. Robust and flexible strain sensors based on dual physically cross-linked double network hydrogels for monitoring human-motion. *Chem. Eng. J.* **2018**, 354, 817–824.
- (45) Li, X.; Yang, Q.; Zhao, Y.; Long, S.; Zheng, J. Dual physically crosslinked double network hydrogels with high toughness and self-healing properties. *Soft Matter* **2017**, *13* (5), 911–920.
- (46) Wang, X.-H.; Song, F.; Qian, D.; He, Y.-D.; Nie, W.-C.; Wang, X.-L.; Wang, Y.-Z. Strong and tough fully physically crosslinked double network hydrogels with tunable mechanics and high self-healing performance. *Chem. Eng. J.* 2018, 349, 588–594.
- (47) Hussain, I.; Sayed, S. M.; Liu, S.; Oderinde, O.; Yao, F.; Fu, G. Glycogen-based self-healing hydrogels with ultra-stretchable, flexible, and enhanced mechanical properties via sacrificial bond interactions. *Int. J. Biol. Macromol.* **2018**, *117*, 648–658.

(48) Li, H.; Wang, H.; Zhang, D.; Xu, Z.; Liu, W. A highly tough and stiff supramolecular polymer double network hydrogel. *Polymer* **2018**, 153, 193–200.

- (49) Li, X.; Wang, H.; Li, D.; Long, S.; Zhang, G.; Wu, Z. Dual Ionically Cross-linked Double-Network Hydrogels with High Strength, Toughness, Swelling Resistance, and Improved 3D Printing Processability. ACS Appl. Mater. Interfaces 2018, 10 (37), 31198—31207.
- (50) Gan, S.; Xu, B.; Zhang, X.; Zhao, J.; Rong, J. Chitosan derivative-based double network hydrogels with high strength, high fracture toughness and tunable mechanics. *Int. J. Biol. Macromol.* **2019**, 137, 495–503.
- (51) Yu, Z. L.; Zeng, W. C.; Zhang, W. H.; Liao, X. P.; Shi, B. Effect of ultrasonic pretreatment on kinetics of gelatin hydrolysis by collagenase and its mechanism. *Ultrason. Sonochem.* **2016**, *29*, 495–501
- (52) Faghihi, S.; Karimi, A.; Jamadi, M.; Imani, R.; Salarian, R. Graphene oxide/poly(acrylic acid)/gelatin nanocomposite hydrogel: experimental and numerical validation of hyperelastic model. *Mater. Sci. Eng., C* **2014**, *38*, 299–305.
- (53) Wu, T.; Xu, Z.; Zhang, Y.; Wang, H.; Cui, C.; Chang, B.; Feng, X.; Liu, W. A pH-Responsive Biodegradable High-Strength Hydrogel as Potential Gastric Resident Filler. *Macromol. Mater. Eng.* **2018**, 303 (10), 1800290.
- (54) Suo, H.; Zhang, D.; Yin, J.; Qian, J.; Wu, Z. L.; Fu, J. Interpenetrating polymer network hydrogels composed of chitosan and photocrosslinkable gelatin with enhanced mechanical properties for tissue engineering. *Mater. Sci. Eng., C* **2018**, 92, 612–620.
- (55) Zhao, X.; Lang, Q.; Yildirimer, L.; Lin, Z. Y.; Cui, W.; Annabi, N.; Ng, K. W.; Dokmeci, M. R.; Ghaemmaghami, A. M.; Khademhosseini, A. Photocrosslinkable Gelatin Hydrogel for Epidermal Tissue Engineering. *Adv. Healthcare Mater.* **2016**, 5 (1), 108–18.
- (56) Feng, Q.; Wei, K.; Lin, S.; Xu, Z.; Sun, Y.; Shi, P.; Li, G.; Bian, L. Mechanically resilient, injectable, and bioadhesive supramolecular gelatin hydrogels crosslinked by weak host-guest interactions assist cell infiltration and in situ tissue regeneration. *Biomaterials* **2016**, *101*, 217–28.
- (57) Hou, J.; Ren, X.; Guan, S.; Duan, L.; Gao, G. H.; Kuai, Y.; Zhang, H. Rapidly recoverable, anti-fatigue, super-tough double-network hydrogels reinforced by macromolecular microspheres. *Soft Matter* **2017**, *13* (7), 1357–1363.
- (58) Huang, J.; Zhao, L.; Wang, T.; Sun, W.; Tong, Z. NIR-Triggered Rapid Shape Memory PAM-GO-Gelatin Hydrogels with High Mechanical Strength. *ACS Appl. Mater. Interfaces* **2016**, 8 (19), 12384–92.
- (59) Yan, X.; Yang, J.; Chen, F.; Zhu, L.; Tang, Z.; Qin, G.; Chen, Q.; Chen, G. Mechanical properties of gelatin/polyacrylamide/graphene oxide nanocomposite double-network hydrogels. *Compos. Sci. Technol.* **2018**, *163*, 81–88.
- (60) Tang, Q.; Wu, J.; Lin, J.; Fan, S.; Hu, D. A multifunctional poly(acrylic acid)/gelatin hydrogel. *J. Mater. Res.* **2009**, 24 (05), 1653–1661.
- (61) Nakayama, A.; Kakugo, A.; Gong, J. P.; Osada, Y.; Takai, M.; Erata, T.; Kawano, S. High Mechanical Strength Double-Network Hydrogel with Bacterial Cellulose. *Adv. Funct. Mater.* **2004**, *14* (11), 1124–1128.
- (62) Meng, Z. X.; Wang, Y. S.; Ma, C.; Zheng, W.; Li, L.; Zheng, Y. F. Electrospinning of PLGA/gelatin randomly-oriented and aligned nanofibers as potential scaffold in tissue engineering. *Mater. Sci. Eng., C* **2010**, *30* (8), 1204–1210.
- (63) Baroudi, I.; Simonnet-Jégat, C.; Roch-Marchal, C.; Leclerc-Laronze, N.; Livage, C.; Martineau, C.; Gervais, C.; Cadot, E.; Carn, F.; Fayolle, B.; Steunou, N. Supramolecular Assembly of Gelatin and Inorganic Polyanions: Fine-Tuning the Mechanical Properties of Nanocomposites by Varying Their Composition and Microstructure. *Chem. Mater.* **2015**, 27 (5), 1452–1464.
- (64) Naseri, N.; Deepa, B.; Mathew, A. P.; Oksman, K.; Girandon, L. Nanocellulose-Based Interpenetrating Polymer Network (IPN)

Macromolecules

Hydrogels for Cartilage Applications. *Biomacromolecules* **2016**, *17* (11), 3714–3723.

- (65) Li, N.; Chen, W.; Chen, G.; Tian, J. Rapid shape memory TEMPO-oxidized cellulose nanofibers/polyacrylamide/gelatin hydrogels with enhanced mechanical strength. *Carbohydr. Polym.* **2017**, *171*, 77–84.
- (66) He, Q.; Huang, Y.; Wang, S. Hofmeister Effect-Assisted One Step Fabrication of Ductile and Strong Gelatin Hydrogels. *Adv. Funct. Mater.* **2018**, 28 (5), 1705069.
- (67) Liang, J.; Guo, Z.; Timmerman, A.; Grijpma, D.; Poot, A. Enhanced mechanical and cell adhesive properties of photocrosslinked PEG hydrogels by incorporation of gelatin in the networks. *Biomed Mater.* **2019**, *14* (2), 024102.
- (68) Giuseppe, M. D.; Law, N.; Webb, B.; Macrae, R. A.; Liew, L. J.; Sercombe, T. B.; Dilley, R. J.; Doyle, B. J. Mechanical behaviour of alginate-gelatin hydrogels for 3D bioprinting. *J. Mech Behav Biomed Mater.* **2018**, *79*, 150–157.
- (69) Sudre, G.; Olanier, L.; Tran, Y.; Hourdet, D.; Creton, C. Reversible adhesion between a hydrogel and a polymer brush. *Soft Matter* **2012**, *8* (31), 8184–8193.
- (70) Gong, J. P.; Katsuyama, Y.; Kurokawa, T.; Osada, Y. Double-Network hydrogels with extremely high mechanical strength. *Adv. Mater.* **2003**, *15*, 1155–1158.
- (71) Chen, H.; Zhao, C.; Zhang, M.; Chen, Q.; Ma, J.; Zheng, J. Molecular Understanding and Structural-Based Design of Polyacrylamides and Polyacrylates as Antifouling Materials. *Langmuir* **2016**, 32 (14), 3315–30.
- (72) Xin, H.; Saricilar, S. Z.; Brown, H. R.; Whitten, P. G.; Spinks, G. M. Effect of First Network Topology on the Toughness of Double Network Hydrogels. *Macromolecules* **2013**, *46* (16), 6613–6620.